Supporting Information (SI) for:

Ta-Doped Porous TiO_2 Nanorods Arrays by Substrate-Assisted Synthesis: Efficient Photoelectrocatalysts for Water Oxidation

Shiman He,[a] Yuying Meng,[*,a] Qili Wu,[a] Jingling Yang,[a] Senchuan Huang,[a] Xiaohui Li,[a] Shengfu Tong,[a] Tewodros Asefa,[*, b] and Mingmei Wu[*,a]

[a] MOE Key Laboratory of Bioinorganic and Synthetic Chemistry, School of Chemistry, Sun Yat-Sen University, No. 135, Xingang Xi Road, Guangzhou 510275, P. R. China

[b] Department of Chemistry and Chemical Biology and Department of Chemical and Biochemical Engineering, Rutgers, The State University of New Jersey, 610 Taylor Road, Piscataway, New Jersey 08854, United States

*** Corresponding Authors:** Yuying Meng: yymeng9169@gmail.com;
Tewodros Asefa: tasefa@chem.rutgers.edu;
Mingmei Wu: ceswmm@mail.sysu.edu.cn

Tantalum foil (0.127 mm thick, purity: 99.95 %) was obtained from Alfa Aesar Co., Ltd. Hydrochloric acid (HCl, 37.5 % wt./wt.), acetone, 2-propanol, *N*,*N*-dimethylformamide and absolute ethanol were purchased from Tianjin Fu Yu Co., Ltd. Tetrabutyl titanate (≥ 99.0 %) was acquired from Aladdin Industrial Corporation. Sodium sulfate (anhydrous) was purchased from Guangzhou Chemical Reagent Factory. Fluorine-doped tin oxide (FTO, 2.2 mm thick, 7 Ω cm^{-2}, Pilkington) was obtained from Solar Energy Technology Co., Ltd, Wuhan Jinge, China. All the materials, chemicals and reagents were of analytical grade and used as received without further purification. Deionized water was used throughout the experiments.

Table S1. Materials synthesized using different synthetic conditions for the studies.

Main Materials (Ta-PTNA-*t*)	Hydrothermal Temperature (°C)	Hydrothermal Time (h)	Calcination Temperature (°C)	Calcination Time (h)
Ta-PTNA-3	180	**3**	450	1
Ta-PTNA-5	180	**5**	450	1
Ta-PTNA-10	180	**10**	450	1
Ta-PTNA-15	180	**15**	450	1
Ta-PTNA-24	180	**24**	450	1
Control Samples, Series A (Ta-PTNA-HT)				
Ta-PTNA-H160	**160**	10	450	1
Ta-PTNA-H200	**200**	10	450	1
Control Samples, Series B (Ta-PTNA-CT)				
Ta-PTNA-C250	180	10	**250**	1
Ta-PTNA-C300	180	10	**300**	1
Ta-PTNA-C350	180	10	**350**	1
Ta-PTNA-C400	180	10	**400**	1
Ta-PTNA-C500	180	10	**500**	1
Ta-PTNA-C550	180	10	**550**	1
Control Samples, Series C (Ta-PTNA-C*t*)				
Ta-PTNA-C*t*0	180	10	450	**0**
Ta-PTNA-C*t*30	180	10	450	**0.5**
Ta-PTNA-C*t*120	180	10	450	**2**

Supplementary Figures and Discussions

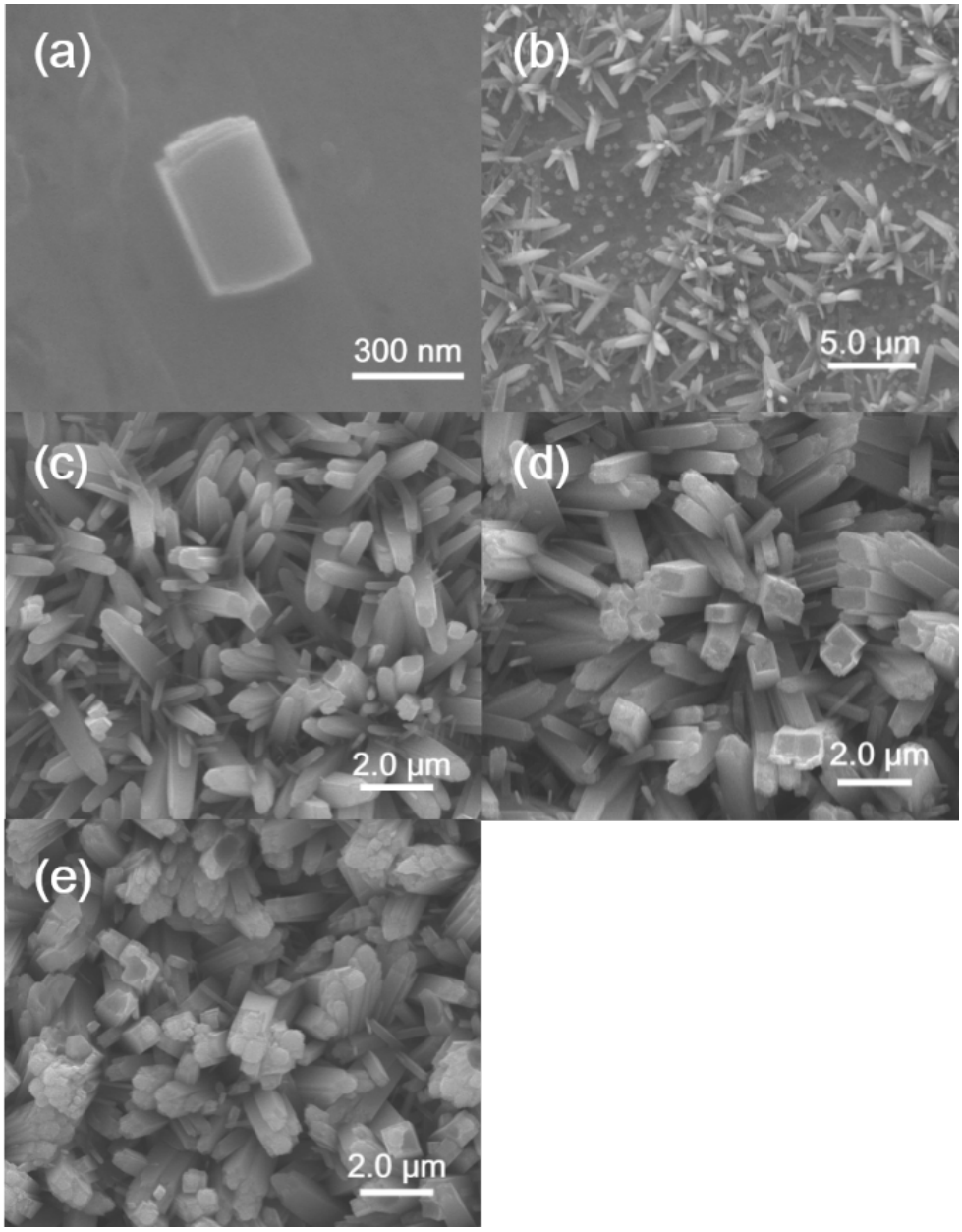

Figure S1. Top view SEM images of hydrothermally grown TiO_2 on Ta foil at 180 °C for (a) 1 h, (b) 3 h, (c) 5 h, (d) 15 h and (e) 24 h before being subjected to calcination.

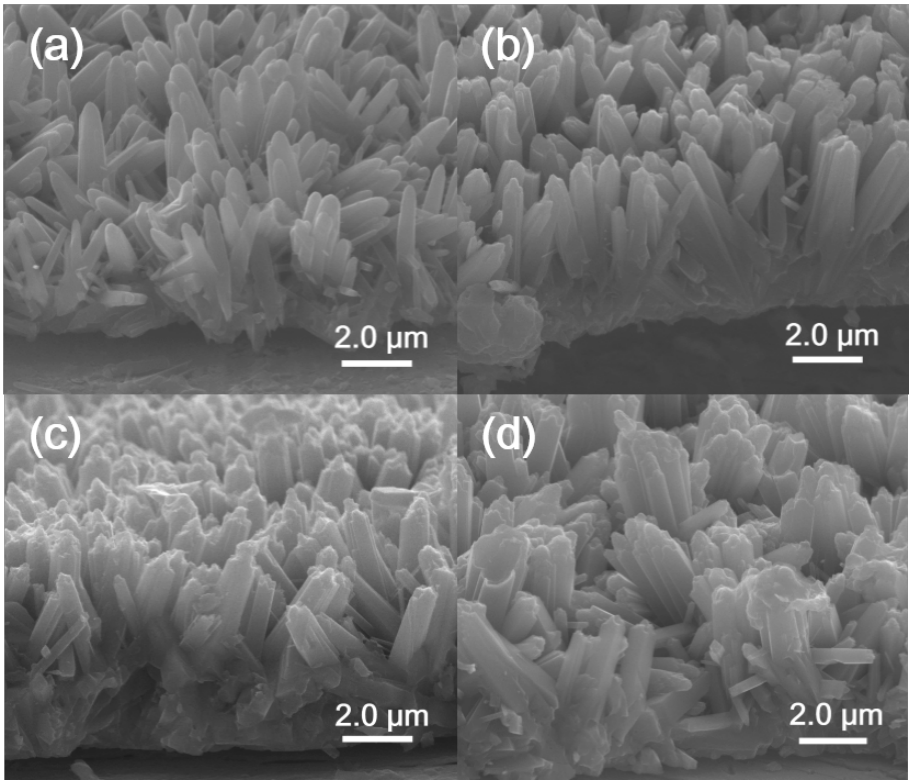

Figure S2. Cross-sectional view SEM images of hydrothermally grown TiO_2 on Ta substrate at 180 °C for (a) 5 h, (b) 10 h, (c) 15 h and (d) 24 h before being subjected to calcination.

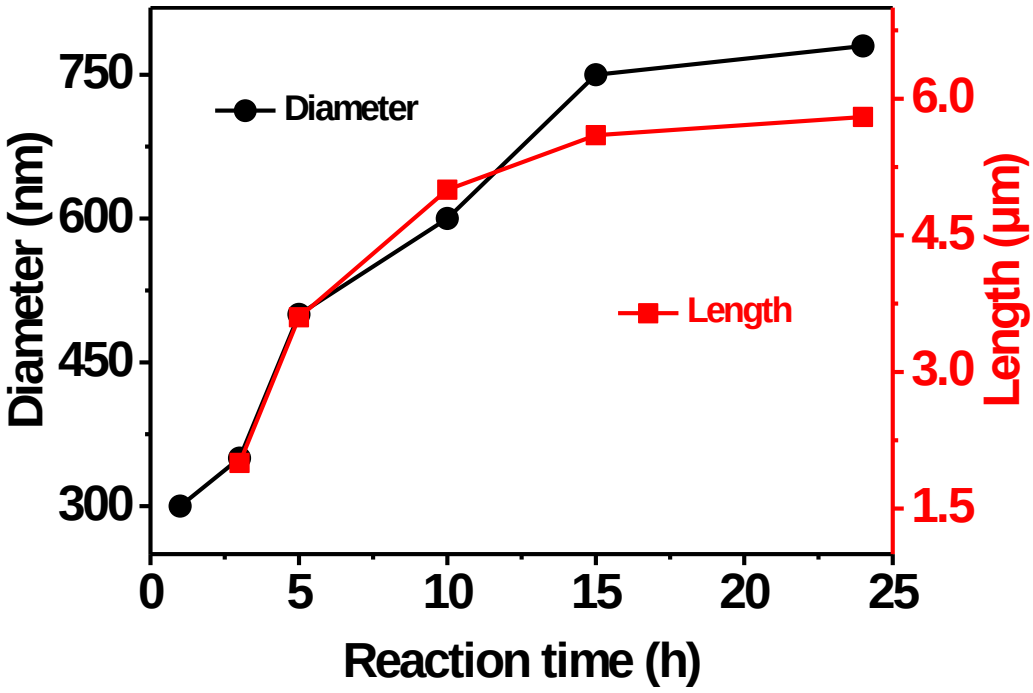

Figure S3. Distribution of mean diameter and length of Ta-doped TiO_2 arrays obtained with hydrothermal treatment at 180 °C for various periods of time.

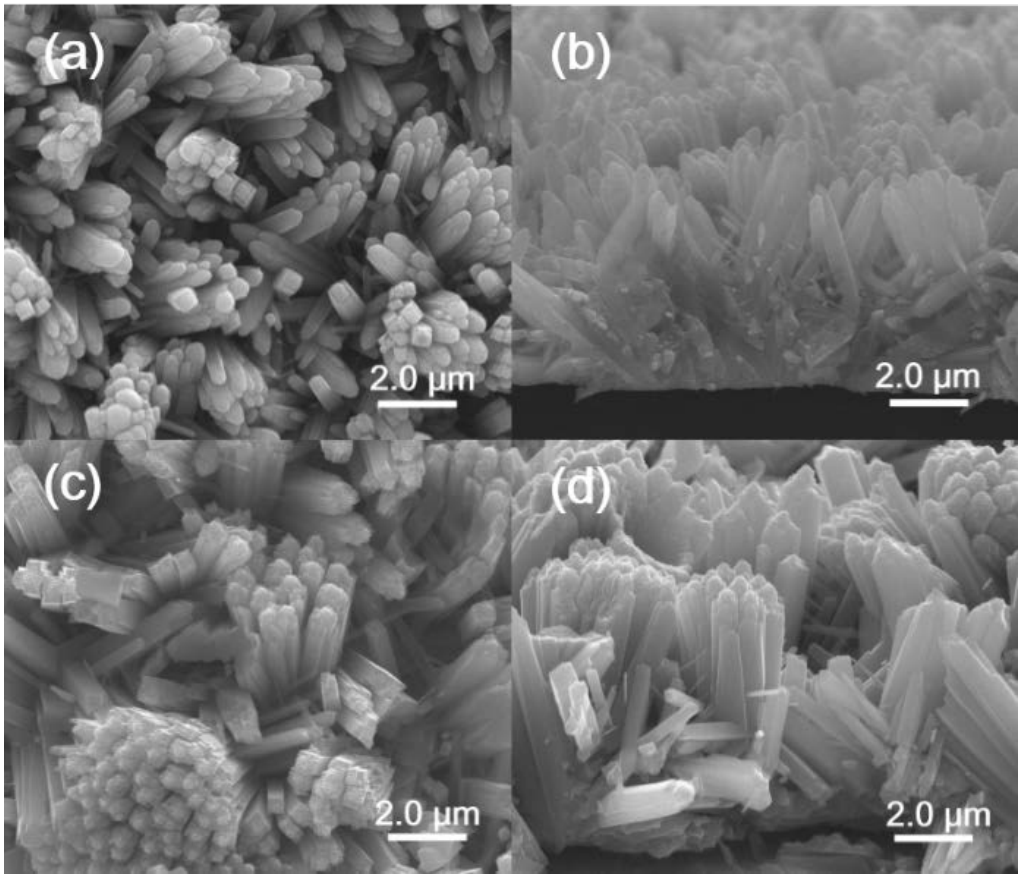

Figure S4. Top view and cross-sectional view SEM images of hydrothermally grown TiO_2 nanorods on Ta foil for 10 h at (a, b) 160 °C and (c, d) 200 °C before being subjected to calcination.

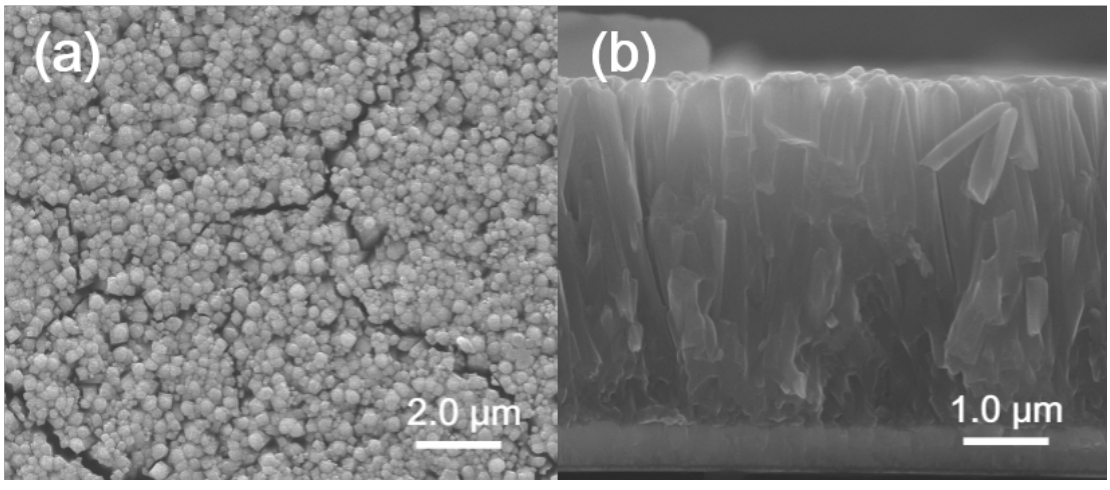

Figure S5. (a) Top view and (b) cross-sectional view SEM images of undoped TiO_2/FTO obtained with hydrothermal reaction at 180 °C for 10 h.

Table S2. SEM-based EDX results for atomic percentage (%) of Ta in the Ta-PTNA-*t* materials obtained with hydrothermal treatment at 180 °C for different periods of time.[a]

Sample	Ta-PTNA-5	Ta-PTNA-10	Ta-PTNA-15	Ta-PTNA-24
1#	2.28	1.34	1.92	2.01
2#	2.44	1.54	2.01	2.24
3#	2.46	1.41	1.87	2.28
4#	2.19	1.52	1.95	1.98
5#	2.18	1.47	2.06	2.17
Mean	2.31	1.46	1.96	2.14

[a] For each sample, five different areas were selected in SEM mapping to get an average value. For the material obtained with 3 h, no information was given because the amount of TiO_2 in the sample was too small to analyze.

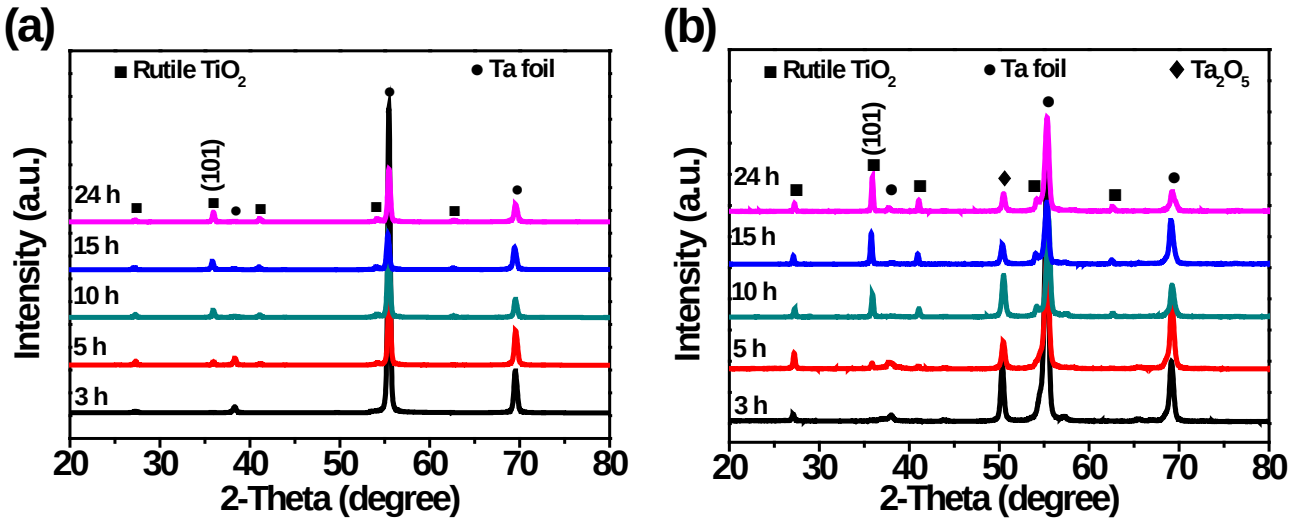

Figure S6. XRD patterns of Ta-PTNA-*t* materials (a) before and (b) after calcination at 450 °C and prior to calcination they were subject to hydrothermal reaction at 180 °C for 3 h (black curves), 5 h (red curves), 10 h (olive curves), 15 h (blue curves) and 24 h (magenta curves).

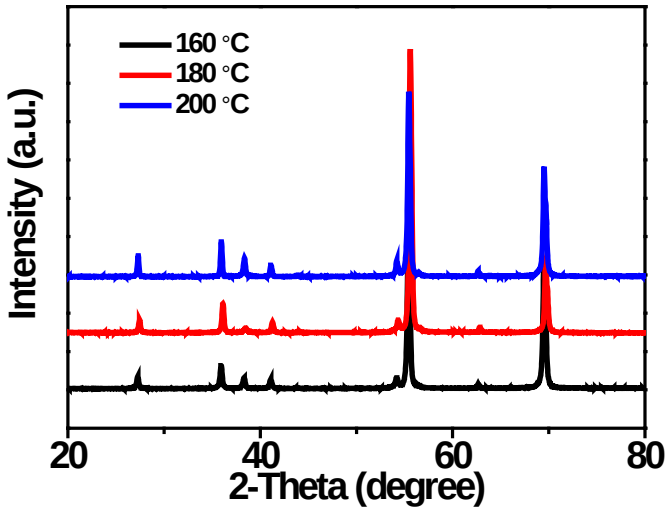

Figure S7. XRD patterns of hydrothermally grown TiO_2 nanorods on Ta foil for 10 h at 160, 180 and 200 °C.

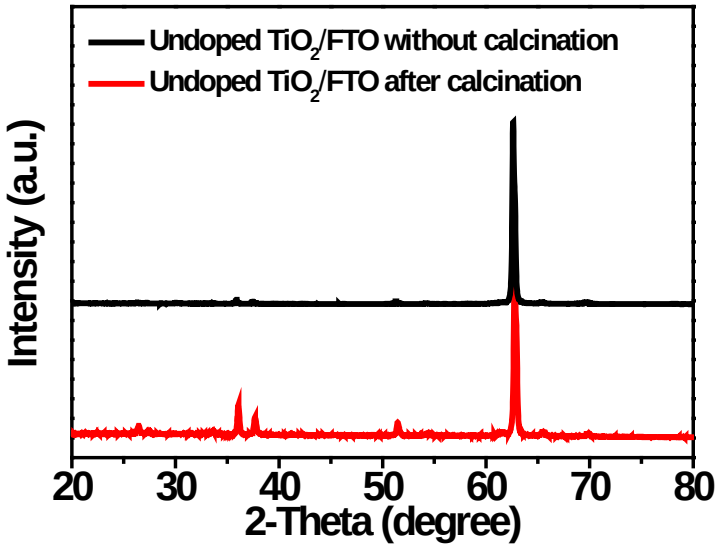

Figure S8. XRD patterns of hydrothermally grown TiO_2 on FTO substrate for 10 h at 180 °C before and after calcination.

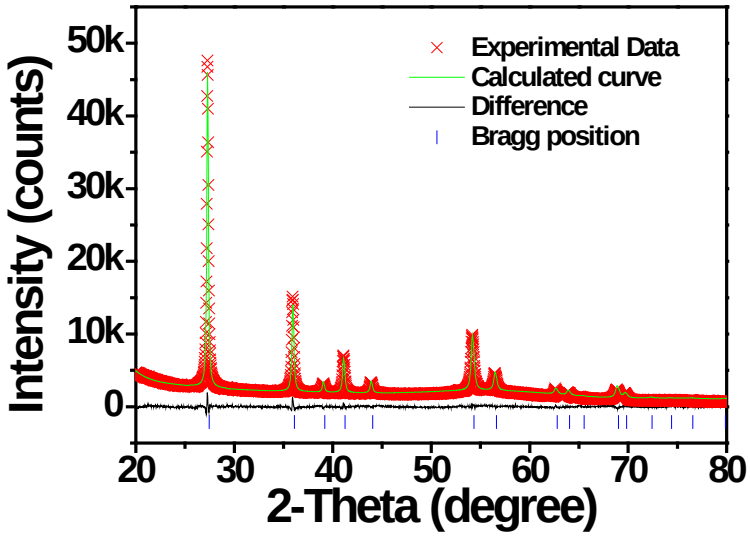

Figure S9. Rietveld refinement plots of XRD analysis of Ta-PTNA-10.

Table S3. Final Rietveld refined structural parameters of Ta-PTNA-10.

Atom	Multiplicity	*X* [a]	*y*	*z*	Occupancy	B_{iso}(Å^2) [b]
Ti	2	0	0	0	0.9850(16)	1
Ta	2	0	0	0	0.0150(16)	1
O	4	0.30476	0.30476	0	1	1

[a] *x*, *y* and *z* represent atom site.

[b] B_{iso} is isotropic temperature factors.

Reliability factor: R_{exp}: 1.99 % R_{wp}: 3.50 % R_p: 2.65 % GOF: 1.76

R_{exp} refers to the experimental *R*-factor, R_{wp} represents the weighted profile *R*-factor, R_p is the pure profile *R*-factor and GOF represents the Goodness of Fit.

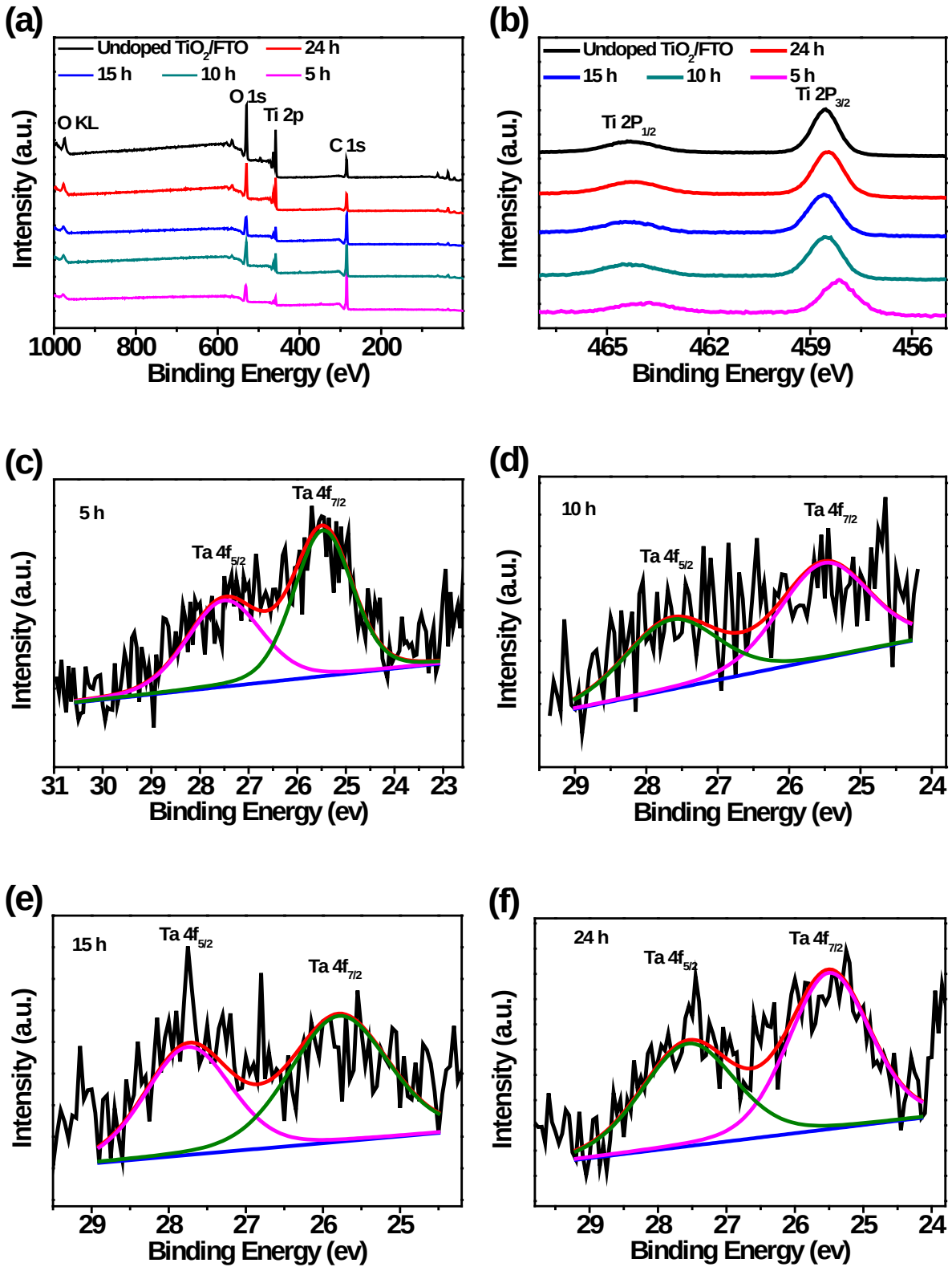

Figure S10. (a) Full-scan XPS and (b) high-resolution Ti 2p XPS spectra of Ta-PTNA-*t* and undoped TiO_2/FTO. (c - f) XPS spectra of Ta 4f of Ta-PTNA-5, -10, -15, and -24, respectively.

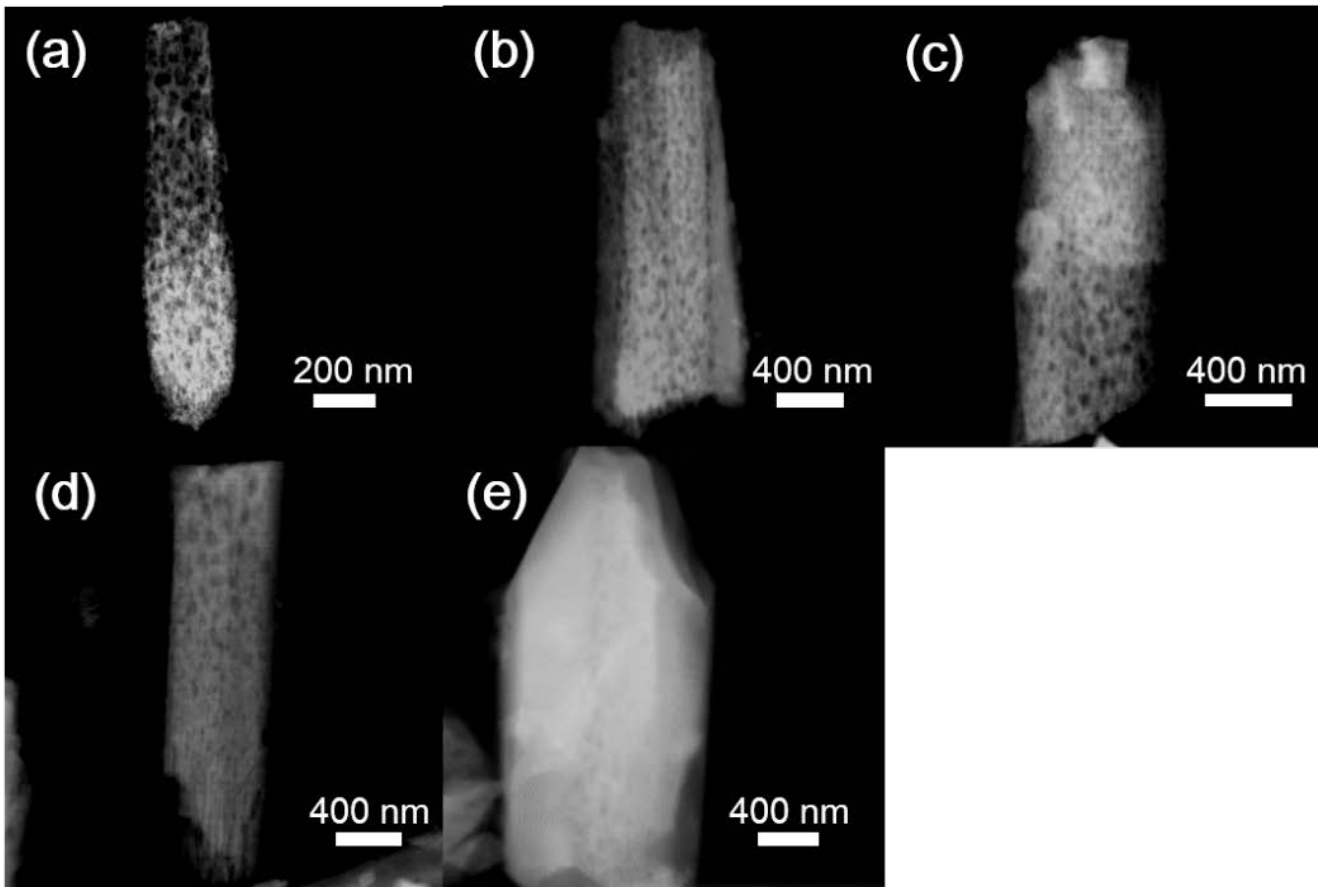

Figure S11. HAADF images of hydrothermally grown porous TiO_2 on Ta foil at 180 °C for (a) 5 h, (b) 10 h, (c) 15 h and (d) 24 h, and (e) undoped TiO_2/FTO.

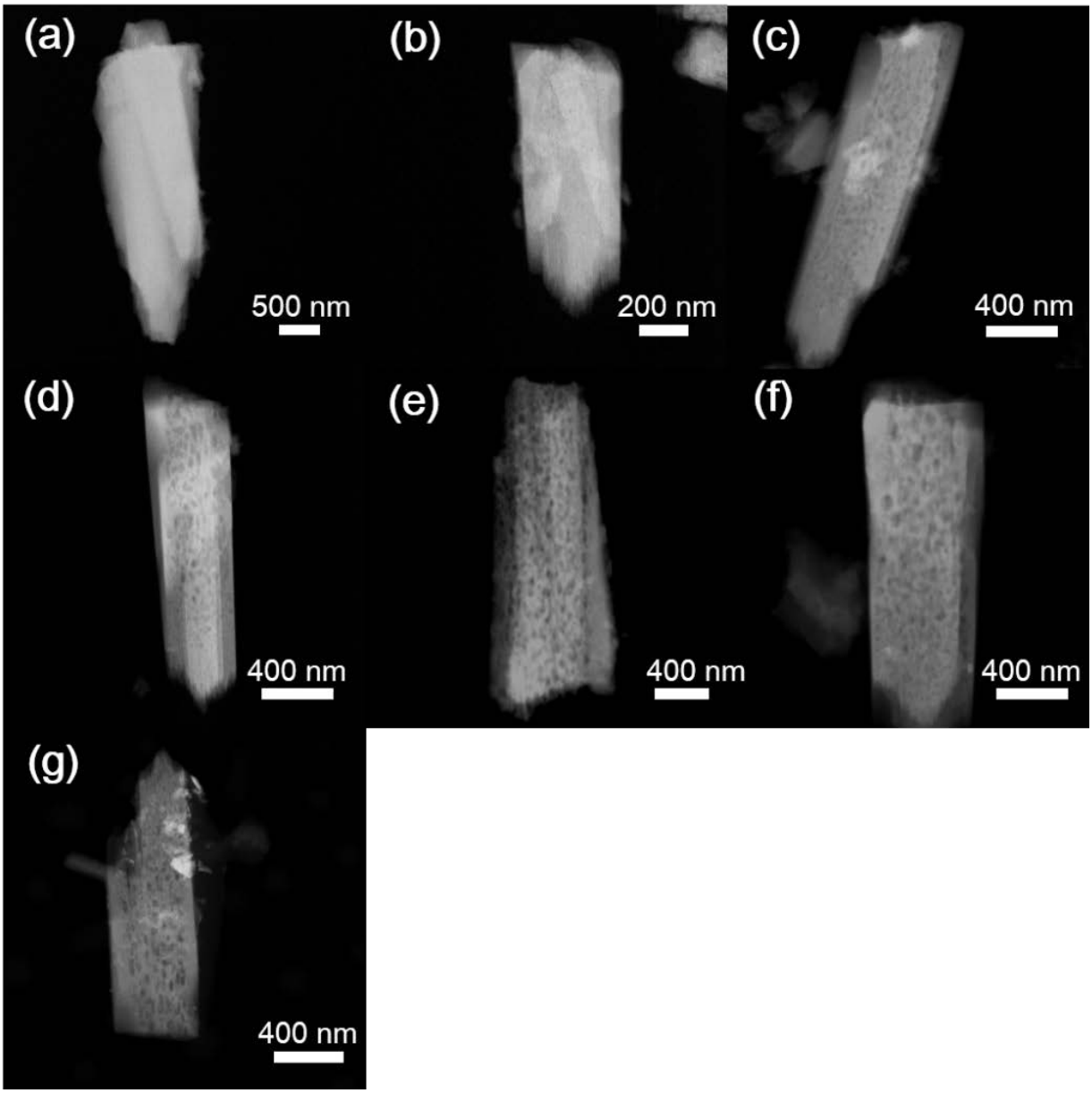

Figure S12. HAADF images of Ta-doped TiO_2 nanorods obtained by hydrothermal treatment at 180 °C for 10 h followed by calcination at (a) 250 °C, (b) 300 °C, (c) 350 °C, (d) 400 °C, (e) 450 °C, (f) 500 °C and (g) 550 °C.

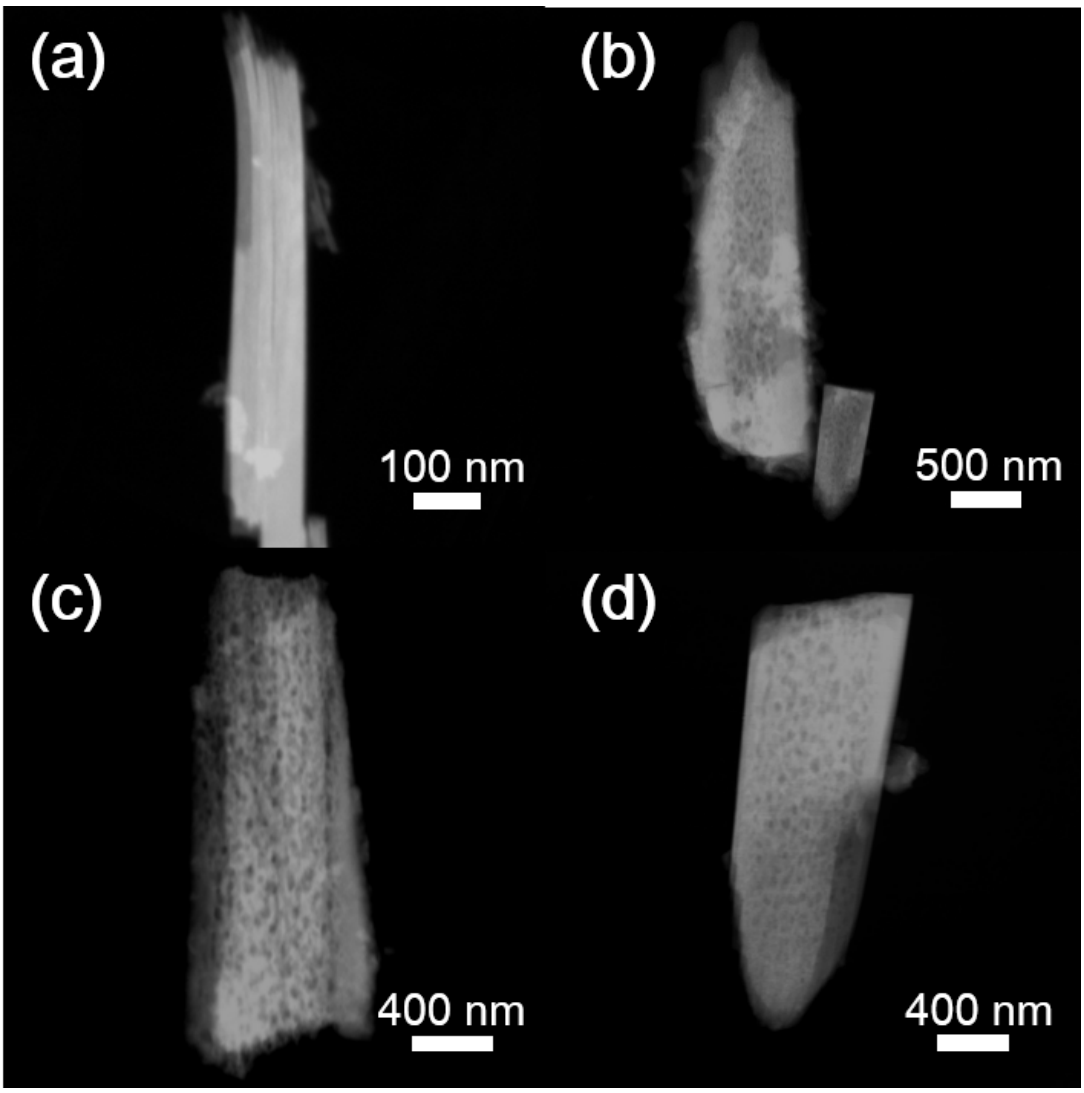

Figure S13. HAADF images of Ta-doped TiO_2 nanorods obtained by hydrothermal treatment at 180 °C for 10 h (a), followed by calcination at 450 °C for (b) 30 min, (c) 60 min and (d) 120 min.

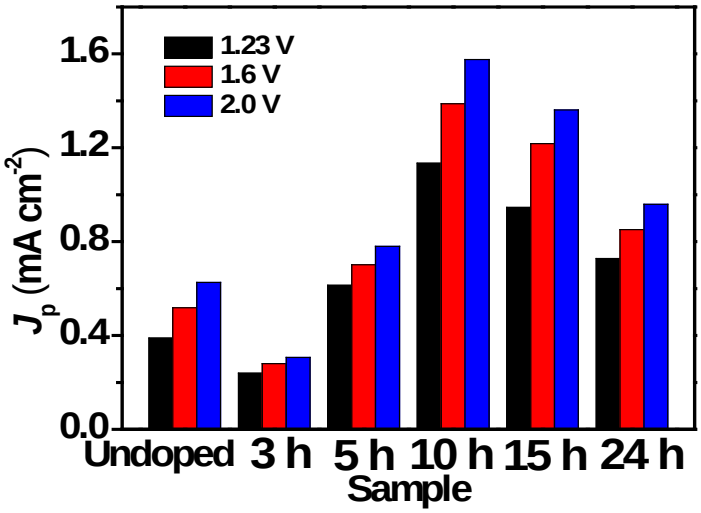

Figure S14. Photocurrent densities of water oxidation at different potentials over undoped TiO_2/FTO and Ta-PTNA-*t* materials.

Table S4. A summary of recent results of photocatalytic performances of various TiO_2-based photoanodes in photoelectrochemical water oxidation.

Photoanode	Photocurrent density (at 1.23 V *vs.* RHE)	Electrolyte	Synthetic Method	Ref.
Rutile TiO_2 nanowires	0.73 mA cm^{-2}	1 M NaOH	Hydrothermal	1
ALD coating TiO_2	1.10 mA cm^{-2}		Atomic layer deposition	
Ti^{3+} self-doped TiO_2	0.70 mA cm^{-2}	1 M KOH	Two-step hydrothermal	2
Branched TiO_2	0.84 mA cm^{-2}	1 M KOH	Hydrothermal	3
Anatase - rutile TiO_2	0.63 mA cm^{-2}	1 M KOH	Magnetron sputtering	4
AZO/TiO_2 nanocones	0.65 mA cm^{-2}	0.1 M Na_2SO_4	Atomic layer deposition	5
AZO/TiO_2/Au NCA	1.10 mA cm^{-2}		Second ALD method	
Ta doped TiO_2 nanotubes	0.53 mA cm^{-2}	1 M KOH	Anodization	6
Ta-PTNA	**1.10 mA cm^{-2}**	**0.2 M Na_2SO_4**	**One-step hydrothermal**	**This work**

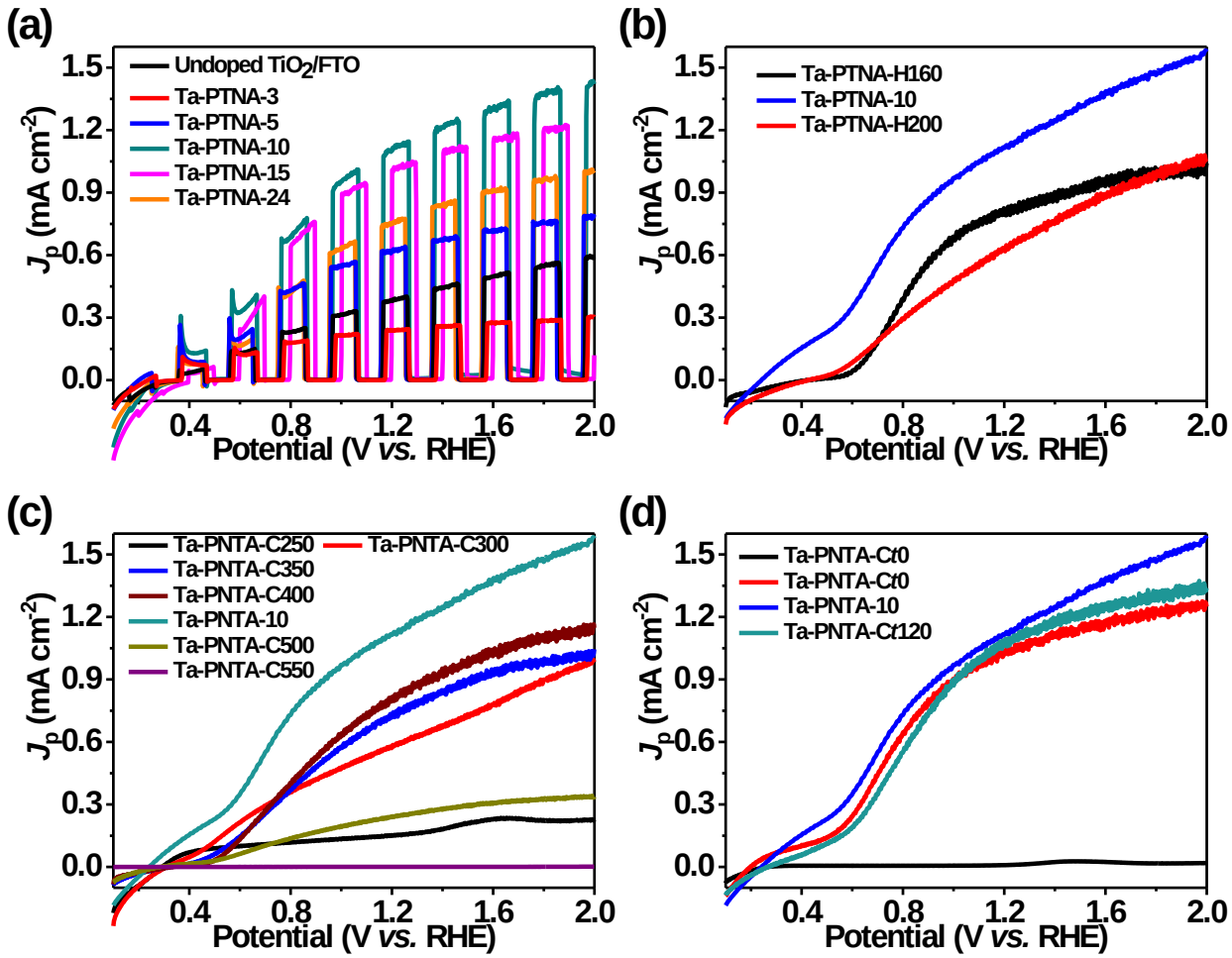

Figure S15. (a) Average chopped linear sweep voltammetry (LSV) curves of Ta-PTNA-*t* and undoped TiO_2/FTO materials at 20 mV s^{-1}. (b) LSV curves of hydrothermally grown TiO_2 nanorods on Ta foil for 10 h at 160, 180 and 200 °C. LSV curves of Ta-doped TiO_2 nanorods obtained by hydrothermal synthesis at 180 °C for 10 h and then (c) calcination at different temperatures for 1 h and (d) calcination at 450 °C for different periods of time.

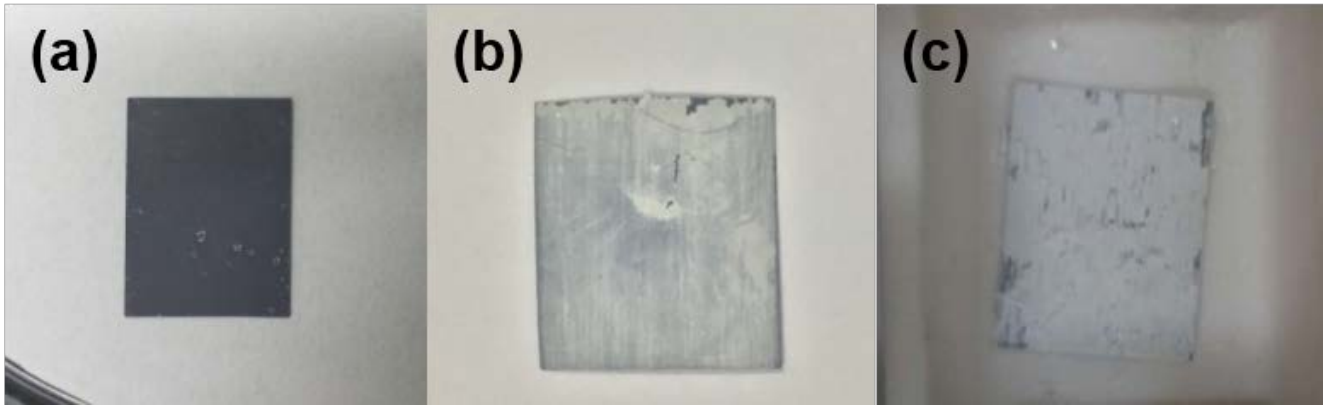

Figure S16. Digital images of Ta-PTNA materials obtained by hydrothermal synthesis at 180 °C for 10 h and then calcination at (a) 450, (b) 500 and 550 °C. The TiO_2 nanorod arrays were partially peeled off from the substrate when the calcination temperature was $\geq$ 500 °C, resulting in their poor PEC catalytic performance toward water oxidation.

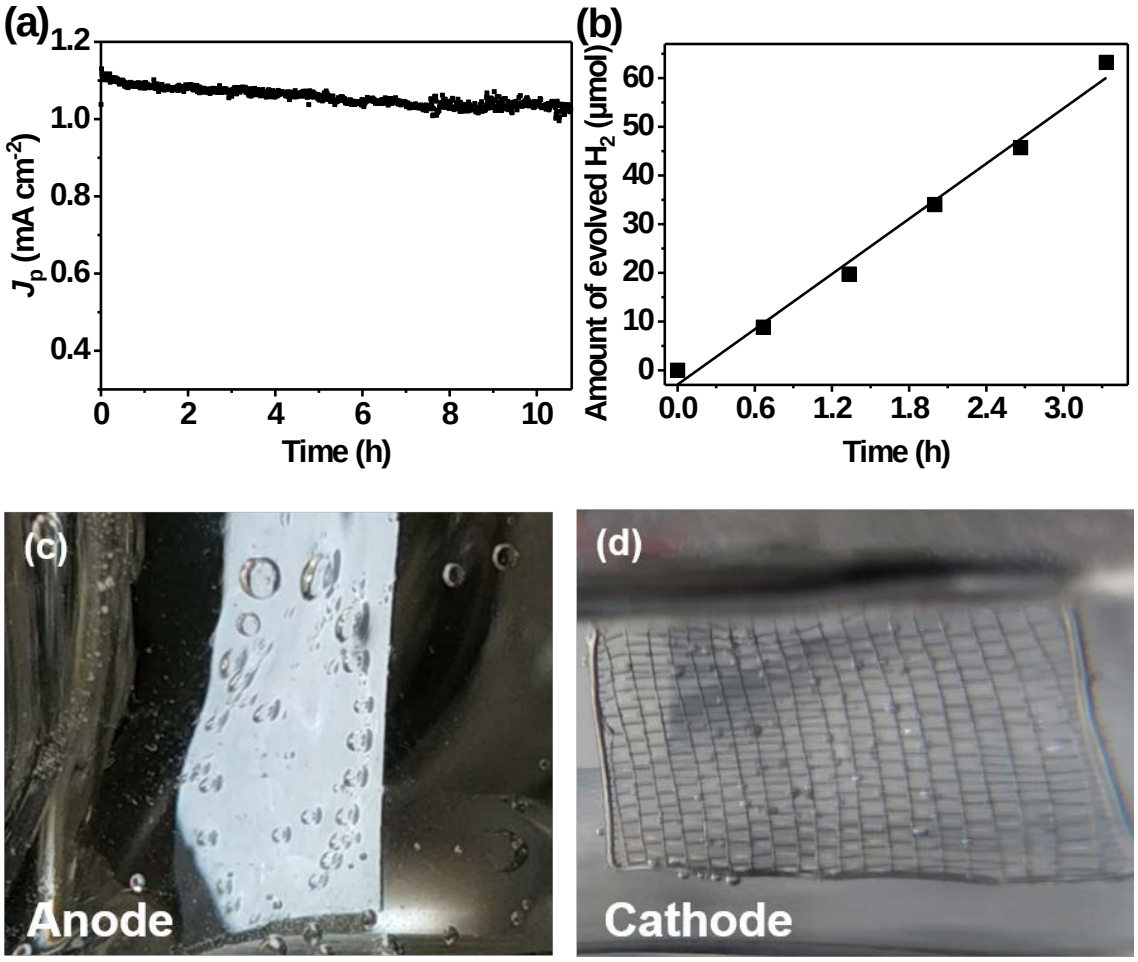

Figure S17. (a) Chronoamperometry curve of water oxidation over Ta-PTNA-10 photoanode at 1.23 V *vs.* RHE in 0.2 M Na_2SO_4. (b) The hydrogen production of Ta-PTNA-10 as a function of reaction time. Photographs of (c) photoanode and (d) cathode during the photoelectrochemical water splitting.

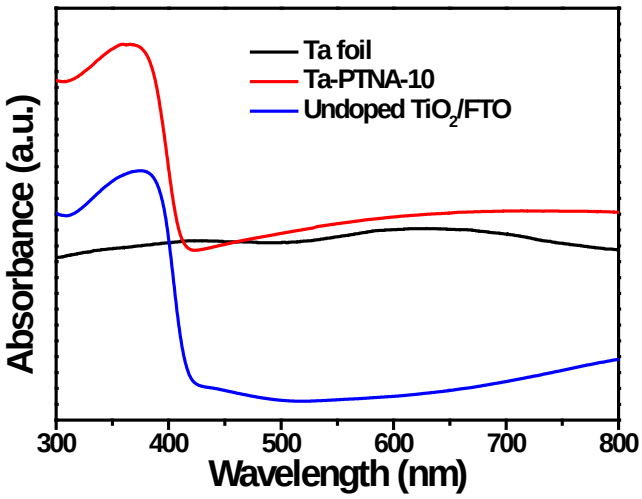

Figure S18. UV-Vis absorption spectra of Ta foil, Ta-PTNA-10 and undoped TiO_2/FTO. The results illustrate that the absorbance in between 420 - 600 nm by Ta-PTNA is mainly due to Ta foil.

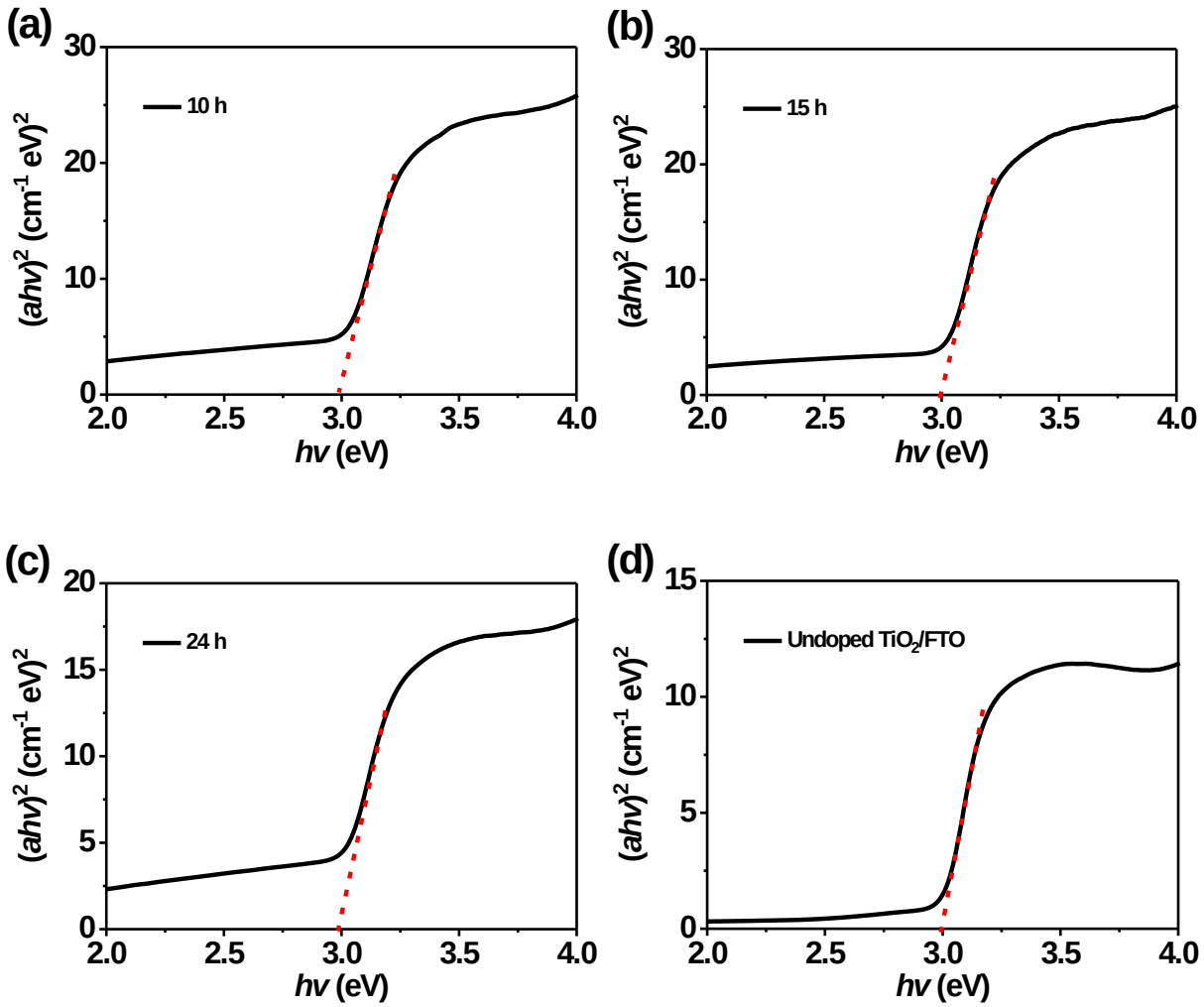

Figure S19. Tauc plots of Ta-PTNA-*t* materials obtained with hydrothermal synthesis at 180 °C for 10 h for (a) 10 h, (b) 15 h, and (c) 24 h, and (d) undoped TiO_2/FTO. Based on the results of UV-Vis absorption spectra and Tauc plots, there is no evidence of a change in band gap in TiO_2 after Ta doping.

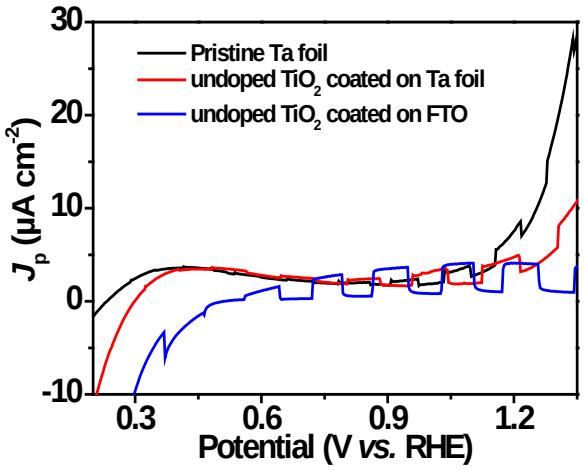

Figure S20. The LSV curves measured under chopped light (AM1.5G) of pristine Ta foil, undoped TiO_2 coated on a Ta foil and undoped TiO_2 coated on a FTO substrate after thermal treatment at 450 °C. Comparable PEC performances were obtained when comparing the result for Ta foil versus that for FTO glass coated with undoped TiO_2 powders, indicating that the absorbance of Ta foil was not crucial to the PEC catalytic performance of Ta-PTNA.

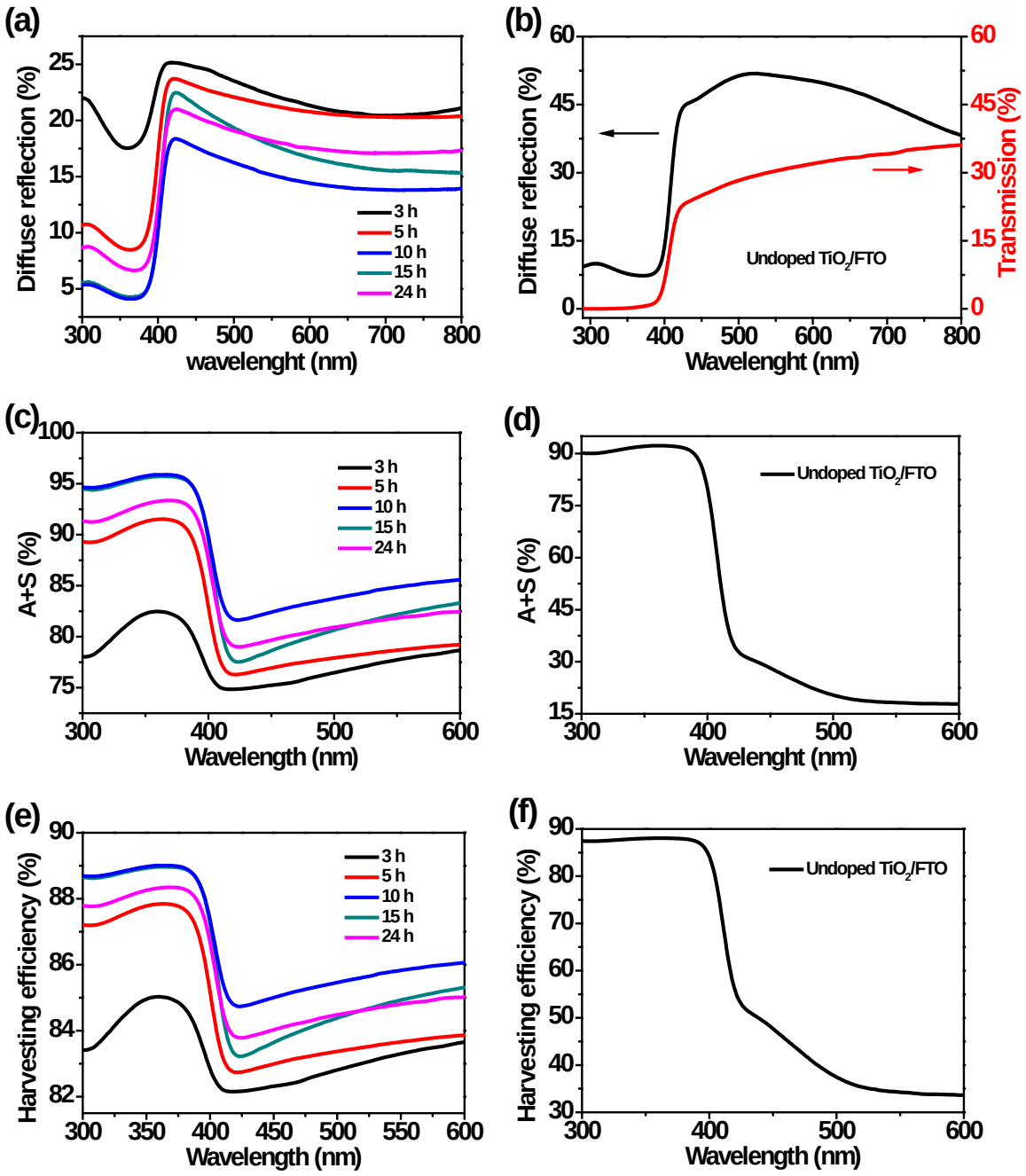

Figure S21. (a) Diffuse reflectance spectra of Ta-PTNA-*t*, (b) Diffuse reflectance and transmission spectra of undoped TiO_2/FTO. UV-Vis absorption properties (η_{abs}) of (c) Ta-PTNA and (d) undoped TiO_2/FTO calculated by using the equation: η_{abs} = Absorption (A) + Scattering (S) = 100 – Transmittance (T) – Reflectance (R).[7] In this case, the transmittance of samples grown on Ta foil is equal to zero because Ta foil is non-transparent. (e-f) The light harvesting efficiencies (η_{LHE}) of Ta-PTNA-*t* and undoped TiO_2/FTO. η_{LHE} was calculated from the absorbance data (η_{abs}) shown in Figure S21c and d: $\eta_{LHE} = (1-10^{-\eta abs}) \times 100\ \%$.[8]

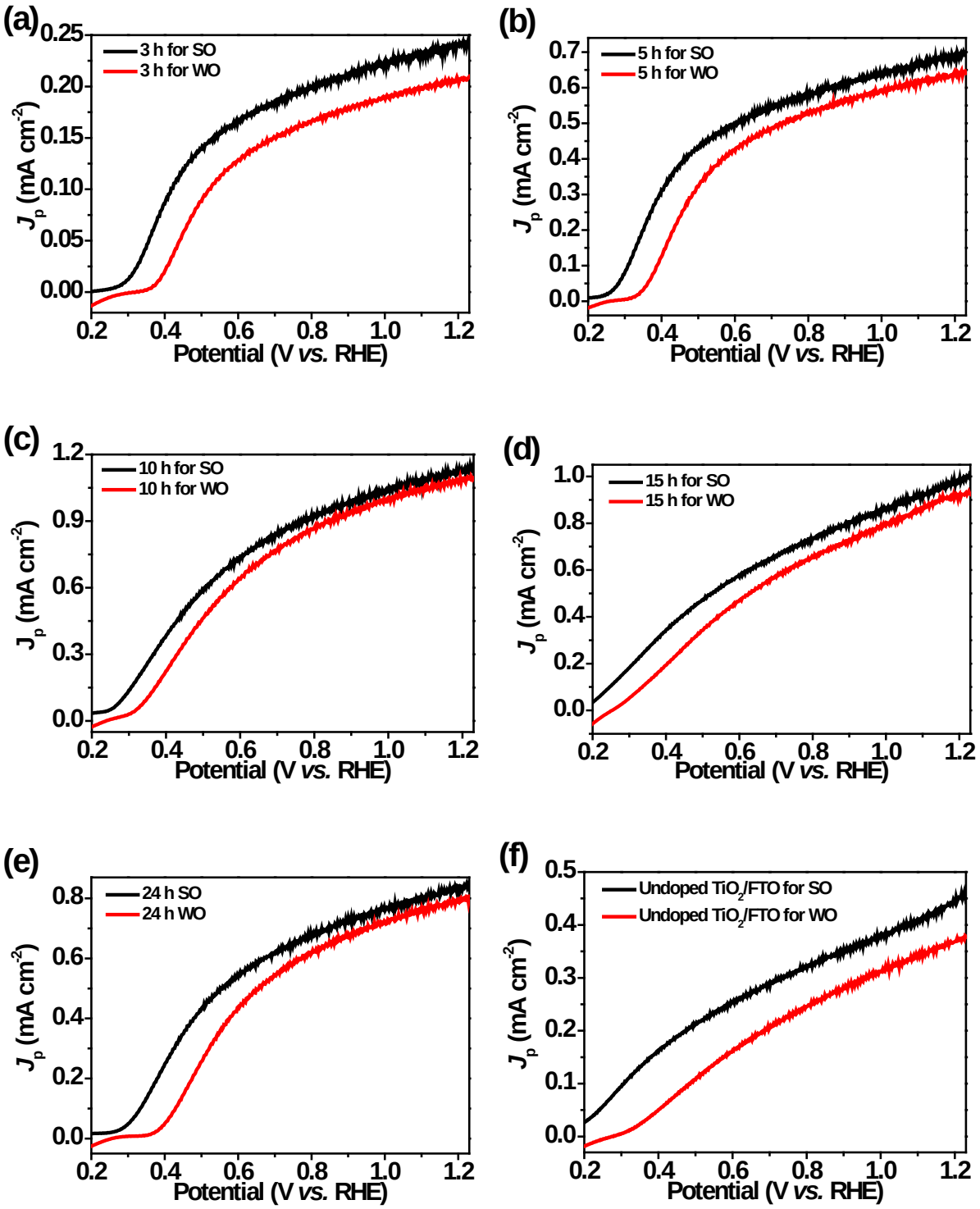

Figure S22. LSV curves of (a-e) Ta-PTNA-*t* and (f) undoped TiO_2/FTO for water oxidation (WO, red line) measured in 0.5 M phosphate buffer (pH = 7) and sulfite oxidation (SO, black line) measured in 0.5 M phosphate buffer in presence of 1 M Na_2SO_3 (pH = 7).

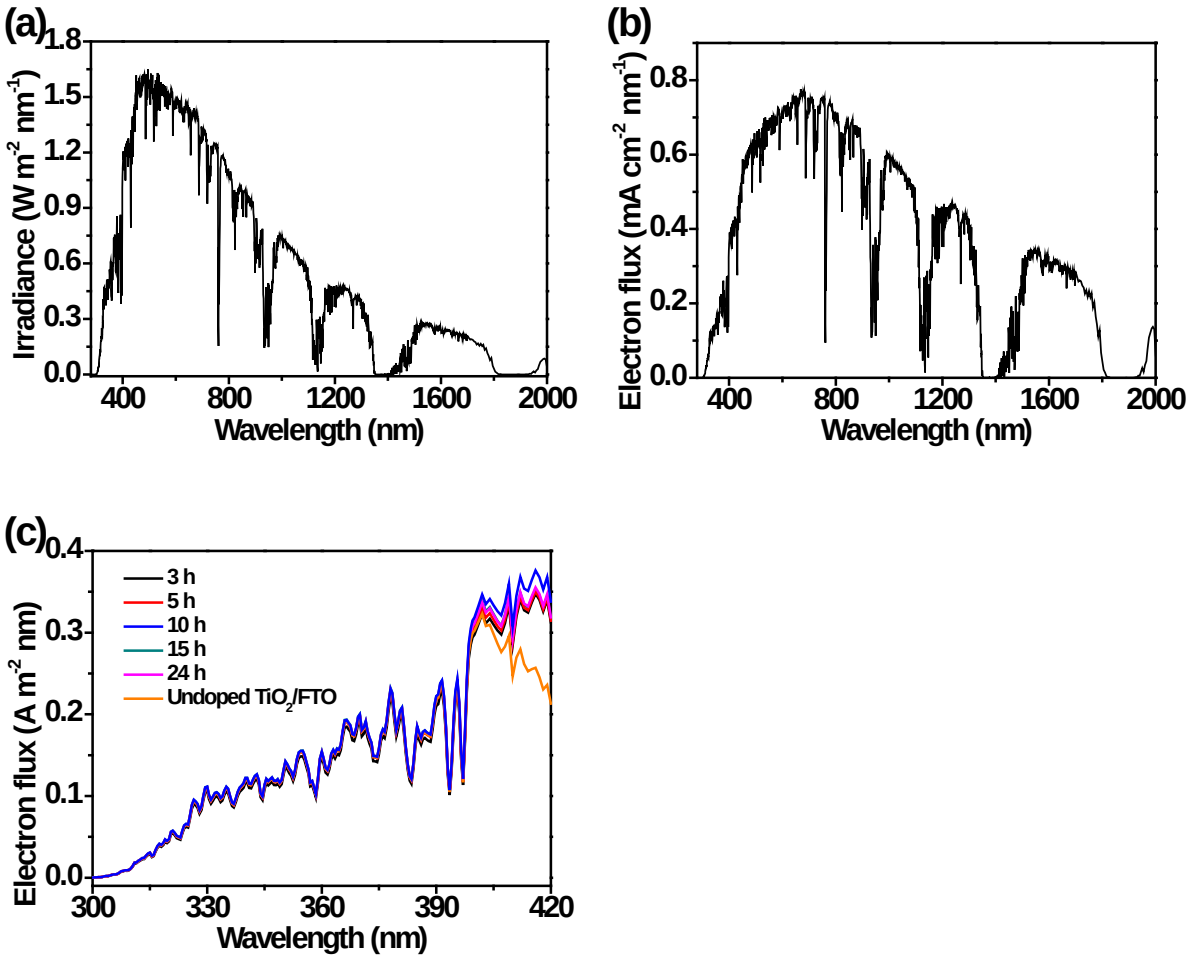

Figure S23. (a) The solar spectral irradiance and (b) electron flux of AM1.5 G solar spectrum. (c) Electro flux of undoped TiO_2/FTO and Ta-PTNA-*t* photoanodes.

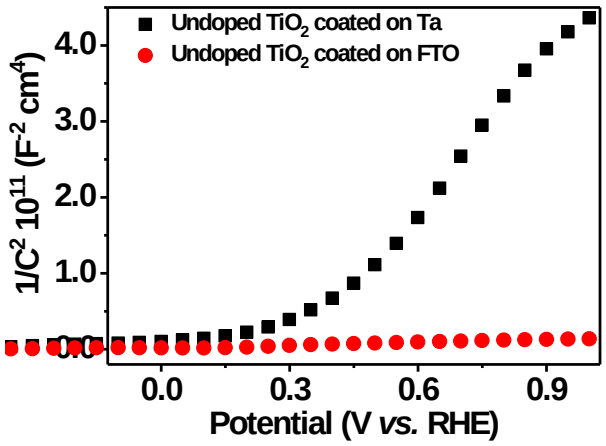

Figure S24. Mott-Schottky plots of scraped undoped TiO_2 coated on Ta foil and FTO.

Based on other reports, it is speculated that TiO_2 should have smaller slope in the M-S plots after Ta doping.[8, 9] However, in our case, the Ta-PTNA-10 possessed relatively larger slope than that of undoped TiO_2/FTO, as illustrated in Figure 5b. In order to explain this novel phenomenon, M-S plots of Ta foil and FTO substrates coated with the same scraped undoped TiO_2 powder (the coating method was described in the synthesis part earlier) were obtained. Figure S24 displays that the undoped TiO_2 coated on FTO has the smaller slope than undoped TiO_2 coated on Ta foil, revealing that the small slope is derived from the substrates rather than Ta dopants. To further probe the improved performance exhibited by the materials after Ta doping, Ta-PTNA-10 powder was scraped from Ta foil and then coated on FTO (using the same coating method). As shown from Figure 5c, Ta-PTNA-10 showed a substantially smaller slope than the undoped material, suggesting that Ta-PTNA-10 has a relatively higher carrier density.

Table S5. Charge carrier density of Ta-doped TiO_2 (Ta-PTNA-10).

Time (h)	**3**	**5**	**10**	**15**	**24**
N_D **(cm^{-3})** [a]	9.92×10^{17}	1.24×10^{18}	2.87×10^{18}	2.11×10^{18}	1.11×10^{18}

[a] N_D represents the donor density, which is calculated using the equation of $N_D = (2 / e\varepsilon\varepsilon_0) / [d(1 / C^2) / dV]$, as mentioned in the Experimental section above.

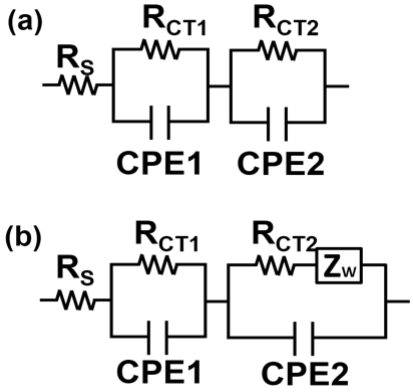

Figure S25. Equivalent circuits used for EIS data fitting (a) with or (b) without Warburg resistance. R_s refers to the solution resistance, R_{CT1} is the charge transfer resistance within the electrode, R_{CT2} represents the resistance to electron transport at the electrode/electrolyte interface, CPE is the constant phase angle element, and Z_W refers to the Warburg resistance.

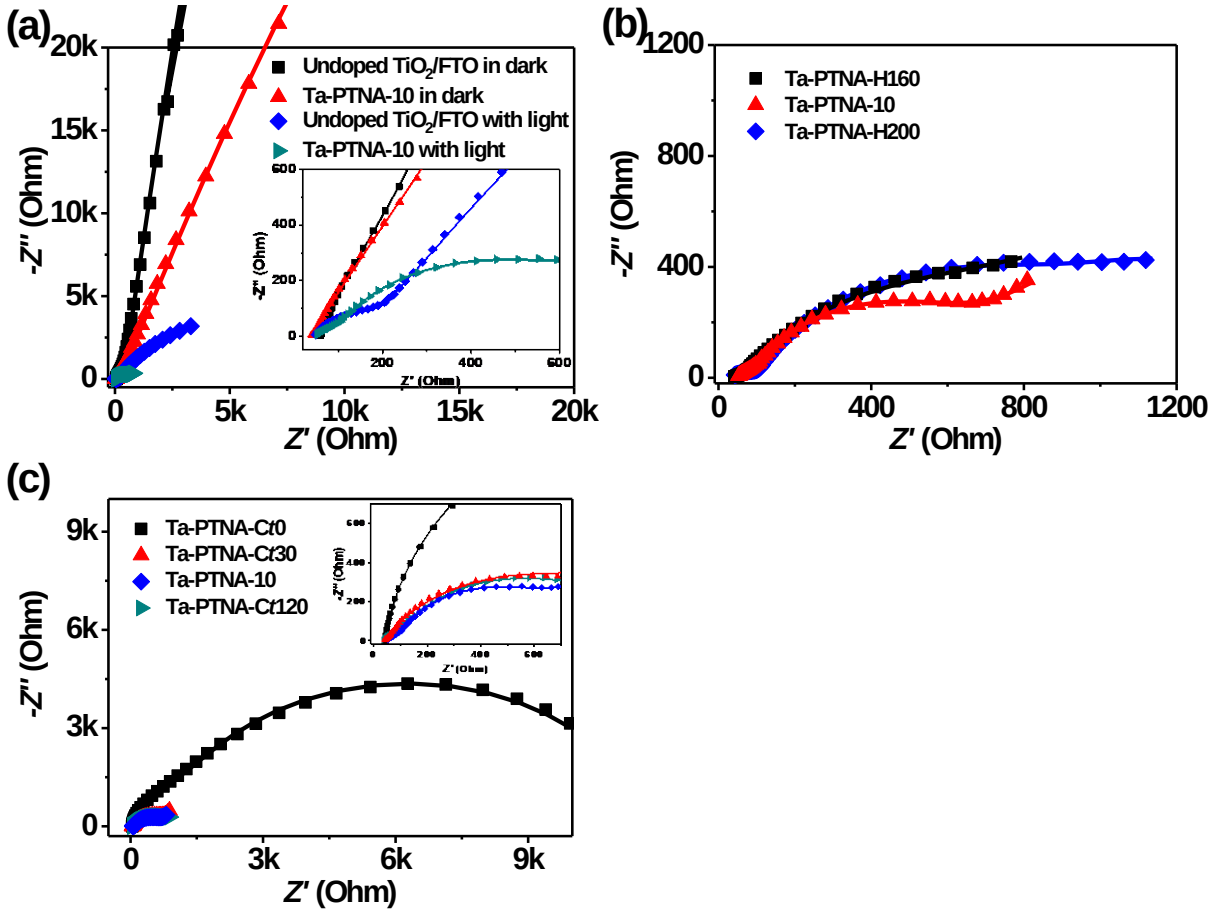

Figure S26. Nyquist plots and magnified Nyquist plots of: (a) Ta-PTNA-10 and undoped TiO_2/FTO with or without illumination. Nyquist plots of Ta-doped porous TiO_2 nanorods obtained (b) at different hydrothermal temperatures for 10 h, (c) calcined at 450 °C for different periods of time. The experimental data and simulated impedance response are represented by discrete points and solid lines, respectively.

Table S6. The values of R and CPE derived by fitting the EIS of undoped TiO_2/FTO and Ta-PTNA-5, -10, -15, -24, recorded as Nyquist plots in 0.2 M Na_2SO_4 at open circle potential under AM1.5G illumination.

Samples	R_S (ohm)	R_{CT1} (ohm)	CPE1-Y_0 (μF)	R_{CT2} (ohm)	CPE2-Y_0 (μF)	W-Y_0 (ohm^{-1} $s^{0.5}$)
Undoped TiO_2/FTO	47.05	126.2	32.04	1133	201.3	/
Ta-PTNA-3	33.88	538	14.51	25250	69.3	/
Ta-PTNA-5	34.89	32.81	4627	2019	145.5	0.001437
Ta-PTNA-10	**48.31**	**58.16**	**221.1**	**451.8**	**270.2**	**0.002491**
Ta-PTNA-15	19.27	83.03	198	512.6	24.67	0.001867
Ta-PTNA-24	28.82	242.9	624.2	983.8	474.3	0.0008087

Table S7. The values of R and CPE derived by fitting the EIS of undoped TiO_2/FTO and Ta-PTNA-10, recorded as Nyquist plots in 0.2 M Na_2SO_4 at open circle potential with or without illumination.

Samples	R_S (ohm)	R_{CT1} (ohm)	CPE1-Y_0 (μF)	R_{CT2} (ohm)	CPE2-Y_0 (μF)	W-Y_0 (ohm^{-1} $s^{0.5}$)
Undoped TiO_2/FTO in dark	58.49	344.0	55.38	2317000	16.79	/
Ta-PTNA-10 in dark	38.47	345.7	80.9	572800	14.13	/
Undoped TiO_2/FTO under light	47.05	126.2	32.04	1133	201.3	/
Ta-PTNA-10 under light	**48.31**	**58.16**	**221.1**	**451.8**	**270.2**	**0.002491**

Table S8. The values of R and CPE derived by fitting the EIS of Ta-doped TiO_2 nanorodes synthesized hydrothermally at 180 °C for 10 h and then calcined at different temperature for 2 h.

Samples	R_S (ohm)	R_{CT1} (ohm)	CPE1-Y_0 (μF)	R_{CT2} (ohm)	CPE2-Y_0 (μF)	W-Y_0 (ohm^{-1} $s^{0.5}$)
Ta-PTNA-C250	33.96	223.2	43	733.2	258.7	0.006057
Ta-PTNA-C300	30.12	170.4	102	667.9	270.7	0.004394
Ta-PTNA-C350	31.63	241.7	325.6	461.3	355.6	0.001862
Ta-PTNA-C400	36.48	227.3	440.2	679.6	701.5	0.001521
Ta-PTNA-10 [a]	**48.31**	**58.16**	**221.1**	**451.8**	**270.2**	**0.002491**
Ta-PTNA-C500	45.26	713	42.51	2411	84.87	0.001211

[a] Note that this material is the same as Ta-PTNA-C450.

Table S9. The values of R and CPE derived by fitting the EIS of Ta-doped TiO_2 nanorods obtained hydrothermally at 160, 180, 200 °C for 10 h.

Samples	R_S (ohm)	R_{CT1} (ohm)	CPE1-Y_0 (μF)	R_{CT2} (ohm)	CPE2-Y_0 (μF)	W-Y_0 (ohm^{-1} $s^{0.5}$)
Ta-PTNA-H160	32.39	50.08	1825	825.7	524.3	0.002912
Ta-PTNA-10	**48.31**	**58.16**	**221.1**	**451.8**	**270.2**	**0.002491**
Ta-PTNA-H200	34.54	82.07	134	957.5	256.1	0.003301

Table S10. The values of R and CPE obtained by fitting the EIS of Ta-doped TiO_2 (hydrothermal at 180 °C for 10 h) annealed at 450 °C for 0, 30, 60 and 120 min.

Samples	R_S (ohm)	R_{CT1} (ohm)	CPE1-Y_0 (μF)	R_{CT2} (ohm)	CPE2-Y_0 (μF)	W-Y_0 (ohm^{-1} $s^{0.5}$)
Ta-PTNA-C*t*0	39.8	874.2	20.81	10870	41.53	/
Ta-PTNA-C*t*30	33.25	109.3	5780	617.6	175.6	0.002315
Ta-PTNA-10	**48.31**	**58.16**	**221.1**	**451.8**	**270.2**	**0.002491**
Ta-PTNA-C*t*120	34.34	79.31	390.6	672.7	357.6	0.004256

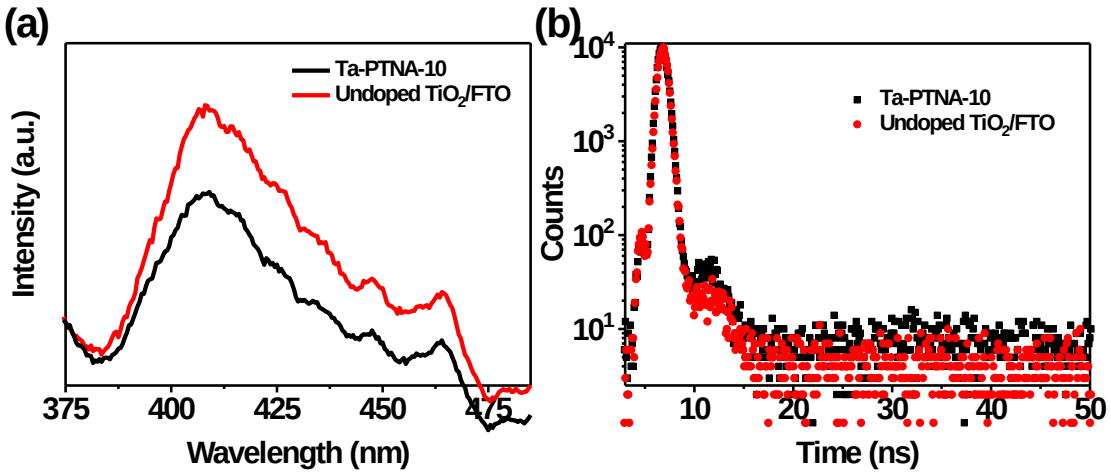

Figure S27. (a) Photoluminescence spectroscopy and (b) time-resolved photoluminescence spectroscopy of Ta-PTNA-10 and undoped TiO_2/FTO materials.

References for Supporting Information Section

1. Y. J. Hwang, C. Hahn, B. Liu and P. D. Yang, *ACS Nano*, 2012, **6**, 5060-5069.
2. C. Y. Mao, F. Zuo, Y. Hou, X. H. Bu and P. Y. Feng, *Angew. Chem. Int. Ed.*, 2014, **53**, 10485-10489.
3. I. S. Cho, Z. B. Chen, A. J. Forman, D. R. Kim, P. M. Rao, T. F. Jaramillo and X. L. Zheng, *Nano Lett.*, 2011, **11**, 4978-4984.
4. A. Li, Z. Wang, H. Yin, S. Wang, P. Yan, B. Huang, X. Wang, R. Li, X. Zong, H. Han and C. Li, *Chem. Sci.*, 2016, **7**, 6076-6082.
5. Y. Mi, L. Wen, R. Xu, Z. Wang, D. Cao, Y. Fang and Y. Lei, *Adv. Energy Mater.*, 2016, **6**, 1501496-1501503.
6. M. Altomare, K. Lee, M. S. Killian, E. Selli and P. Schmuki, *Chem.-Eur. J.*, 2013, **19**, 5841-5844.
7. W. Yang, Y. Yu, M. B. Starr, X. Yin, Z. Li, A. Kvit, S. Wang, P. Zhao and X. Wang, *Nano Lett.*, 2015, **15**, 7574-7580.
8. J. Liu, H. T. Yang, W. W. Tan, X. W. Zhou and Y. A. Lin, *Electrochim. Acta*, 2010, **56**, 396-400.
9. S. Hoang, S. W. Guo and C. B. Mullins, *J. Phys. Chem. C*, 2012, **116**, 23283-23290.